Green Chemistry

PAPER

View Article Online
View Journal

Cite this: DOI: 10.1039/c8gc00208h

Selective production of glycols from xylitol over Ru on covalent triazine frameworks – suppressing decarbonylation reactions†

Anna Katharina Beine,[a] Andreas J. D. Krüger,[a] Jens Artz,[a] Claudia Weidenthaler,[b] Christoph Glotzbach,[c] Peter J. C. Hausoul [a] and Regina Palkovits *[a]

Received 19th January 2018,
Accepted 20th February 2018

DOI: 10.1039/c8gc00208h

rsc.li/greenchem

Ru on covaltent triazine frameworks (CTF) are highly active and selective catalysts for the conversion of xylitol to glycols (80% C-yield) in basic media. With increasing N-content decarbonylation reactions are suppressed leading to high glycol selectivity. The suppression can be attributed to the presence of N in the support and to metal-support interactions. The catalysts exhibit high stability and could be recycled 5 times with minor loss of activity.

Introduction

The use of lignocellulosic biomass for the production of renewable commodity chemicals can decrease the dependence on fossil resources and reduce CO_2 emissions.[1–3] Especially the conversion of non-edible (hemi)cellulose to glycols is a promising route for valorisation (Scheme 1). Ethylene and propylene glycol (EG and PG) are important commodity chemicals that find wide application as monomers and antifreezes and are currently produced from petroleum-based ethylene and propylene. Recent studies have demonstrated that lignocellulosic biomass can be fractionated to insoluble cellulose, soluble lignin and hemicellulose-based sugars.[4] The cellulose fraction can be used for the production of ethanol and platform chemicals such as 5-hydroxymethylfurfural and levulinic acid.[5–7] The hemicellulose fraction, on the other hand, is mainly used to produce furfural.[8] However hemicellulose also possesses great potential for the production of sustainable alkanes and alcohols.[9,10] In particular the selective hydrogenolysis of xylitol (XYL) to glycols represents an interesting reaction in green chemistry.

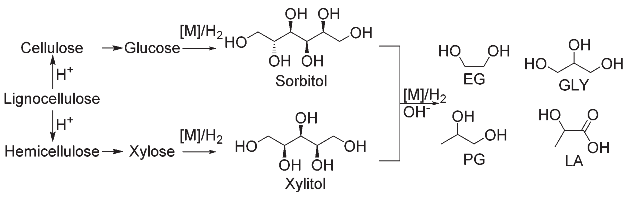

Scheme 1 Production of glycols from biomass *via* metal-catalysed hydrogenolysis.

The conversion of XYL to EG and PG proceeds *via* metal-catalysed dehydrogenation, base-promoted retro-aldol splitting and rehydrogenation.[11–16] Under basic conditions the most important side reaction is the formation of lactic acid (LA).[17] Often used metals in the reaction are Ni, Pt and Ru.[18,19] For Ni-based catalysts different supports and additional metals were used. Ni supported on activated carbon (AC)-$LaOH_3$ enabled the conversion of cellulose to glycols and resulted in a combined yield of 64% while Ni supported on Ce–TiO_2 converted xylitol to glycols with a combined yield of 67%.[20,21] Using a catalyst containing Ni and CaO on carbon Sun *et al.* were able to produce glycols from xylitol with a selectivity of 70%.[19] Ni- and W-containing catalysts on carbon can even facilitate higher selectivity and activity of up to 80% for sugars as well as sugar alcohols.[22–25] Nevertheless, major challenges of these catalysts are leaching, oxidation and agglomeration which lead to an unsatisfactory stability of these catalysts.[24,25] For Pt/C a higher activity was found for the hydrogenolysis of xylitol compared to Pd, Rh and Ru supported on carbon.[18] The obtained selectivity to glycols of 48%, though, was lower than for Ru/C. For the conversion of cellulose also a low glycol selectivity of 24% was reached.[26] The selectivity could be increased to 62% by using a bifunctional Pt and W containing catalyst on carbon support.[26] One drawback of Pt-based catalysts is the high raw material price. For Ru-based catalysts, the

---

[a] *RWTH Aachen University, Worringerweg 2, 52074 Aachen, Germany. E-mail: palkovits@itmc.rwth-aachen.de; Fax: +49 241-80-22177; Tel: +49 241 80 26497*

[b] *Max-Planck-Institut für Kohlenforschung, Kaiser-Wilhelm-Platz 1, 45470 Mülheim, Germany*

[c] *Thyssenkrupp Industrial Solutions AG, ThyssenKrupp Allee 1, 45143 Essen, Germany*

† Electronic supplementary information (ESI) available. See DOI: 10.1039/c8gc00208h

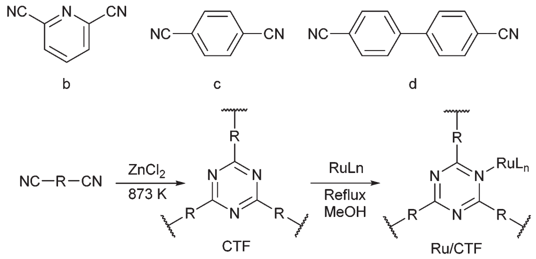

Scheme 2 Monomers for the production of CTF-materials, polymerisation and impregnation.

occurrence of side reactions leads to a wide product spectrum and rather low selectivity.[15,16,27,28]

A common strategy for improving the selectivity of catalysts is variation of the support material. For Ru-based catalysts materials such as AC, carbon nano-fibers (CNF), Al_2O_3, ZrO_2 and TiO_2 were tested. Up to 20% EG and 38% PG was obtained using CNFs, although the formation of LA was not reported.[7,29,30] In addition, doping carbon materials with heteroatoms such as phosphorus and sulfur has been studied for sugar alcohol hydrogenolysis.[31–33] The use of a nickel phosphate phase led to an increase of catalytic activity, while selectivity was only changed minimally. The use of sulfur increased the selectivity for PG to 41% and EG to 26% using sorbitol as substrate. However, the activity decreased significantly and after 4 h only 14% conversion was observed, indicating that S-doping leads to catalyst inhibition.[33] Also in this study the formation of LA was not investigated. Recent studies have shown that N-doping can lead to improved performance in electrochemistry, gas adsorption and separation as well as catalysis.[34–38] Especially, the basic surface properties, high metal dispersion and strong metal–support interactions lead to improved performance and catalyst stability.[33] Recently, covalent triazine frameworks (CTFs) were introduced as tailor-made porous materials with tuneable N-content based on the choice of monomer (Scheme 2).[37] They were used as supports in noble metal-catalysed oxidation reactions and showed a molecular metal dispersion and good stability.[35,38]

CTFs enable a systematic variation of factors assumed crucial for selectivity such as N-content Therefore they were studied in XYL hydrogenolysis and we are able present CTFs as selective support for Ru-based catalysts.

Results and discussion

Catalyst characterisation

CTF-materials based on the monomers, pyridine-2,6-dicarbonitrile (CTF-b), terephthalonitrile (CTF-c) and biphenyl-4,4′-dicarbonitrile (CTF-d) were prepared by polymerization in $ZnCl_2$ at 873 K for 10 h (nomenclature of the CTF-materials was adopted from previous publications).[38] The general synthesis route is shown in Scheme 2.[38] The specific surface areas of the prepared CTF-materials calculated by the BET method range between 1400–1950 m^2 g^{-1} (see Table 1 and Fig. S1 in the ESI†) and are comparable to those reported before.[37,38] The N-content was determined by elemental analysis and varied from 3.7% for CTF-d to 17.2% for CTF-b. The CTF-materials were loaded with 5 wt% Ru by coordination with $[RuCl_2(p\text{-cymene})]_2$ in refluxing methanol.

Table 1 Surface area, total pore volume and elemental analysis for prepared CTF-materials

Catalyst support	S_{BET} [m^2 g^{-1}]	$V_{P(total)}$ [cm^3 g^{-1}]	N-Content [%]
CTF-b	1399	0.92	17.2
CTF-c	1595	0.97	10.4
CTF-d	1949	1.61	3.7

Catalyst screening

Reactions were carried out at 473 K under 8 MPa H_2. $Ca(OH)_2$ was used as base as it was found to be most selective in previous studies.[18] A screening of the most prominent metals (Ni, Pt and Ru) on carbon support was carried out for XYL hydrogenolysis (Table 2). These results are compared to the results of the prepared Ru/CTF catalysts (Fig. 1). All tested carbon sup-

Table 2 Screening of metal on carbon catalysts in the hydrogenolysis of XLY[a]

	Metal loading [wt%]	X (PentOH) [%]	*S* (EG) [%]	*S* (PG) [%]	*S* (GLY) [%]	*S* (LA) [%]
Ni/C	10	100	36	34	2	15
Pt/C	5	97	37	30	13	20
Ru/C	5	100	17	29	1	17

[a] Conditions: 473 K, 3 h, 8 MPa H_2, 2.0 g xylitol, 0.2 g catalyst, 0.3 g $Ca(OH)_2$, 20 mL H_2O. PentOH describes XYL and all other pentitols.

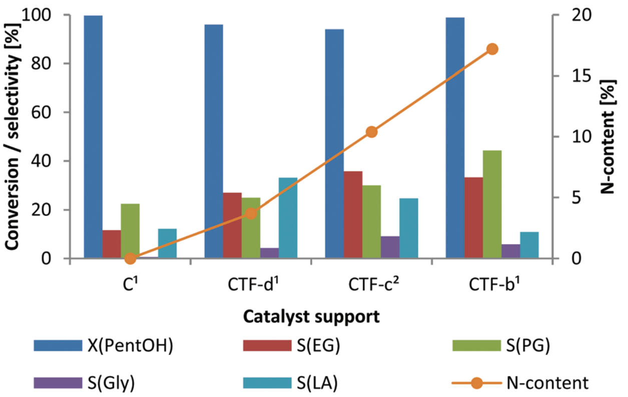

Fig. 1 Influence of the nitrogen content of the support on the Ru-catalysed hydrogenolysis of xylitol (conditions: 473 K, 8 MPa H_2, (1) 4 h, (2) 3 h, 2.0 g xylitol, 0.2 g catalyst, 0.3 g $Ca(OH)_2$, 20 mL H_2O, PentOH describes XYL and all other pentitols).

ported catalysts show close to full conversion of XYL and all other pentitols (PentOH) like ribitol and arabitol after a reaction time of 3 h. The highest selectivity is observed for Pt/C and Ni/C showing a combined glycol selectivity of 67% and 70%, respectively. For Ru/C only low glycol selectivity of 46% is observed. Besides the main products EG and PG, GLY and LA are observed in varying amounts. For Ru/C the HPLC-based mass balance was incomplete indicating the formation of further side products. Extending the reaction time to 4 h leads to a further decrease in glycol selectivity for Ru/C to only 12% for EG and 23% for PG (Fig. 1). In contrast for Ru/CTF-based catalysts the selectivity to glycols is higher and increases with increasing N-content whereas the selectivity to LA decreases. For Ru/CTF-b 36% selectivity to EG and 44% to PG was obtained. This combined glycol selectivity of 80% exceeds the highest selectivity of 67% reached for Ru-based systems by Tronci *et al.* as well as the metal on carbon catalysts investigated above.[33] The selectivity is comparable to Ni and W containing systems that often suffer from leaching.[18–21] It is also noteworthy that the selectivity to LA and GLY is low at 11.1% and 5.8%, respectively.

Product spectrum

Fig. 2 shows the time dependence of the reactions of Ru/C and Ru/CTF-b. In case of Ru/C, PentOH are converted within 2 h of reaction (Fig. 2, left). Initially, EG, PG, GLY and LA are formed with high selectivity but are subsequently consumed and the mass balance decreases rapidly over time. In addition, glycolic acid (GA) was detected as side-product in <1%. The GC data of peracetylated reaction mixtures (Fig. S2 in the ESI†) also reveal the formation of threitol (THR) which, together with GLY and EG, is rapidly consumed. In line with previous observations this indicates the occurrence of decarbonylation reactions.[39] In contrast, for Ru/CTF-b, PentOH are fully converted after 3 h and much higher yields and selectivities are obtained (Fig. 2, right). Only after 4 h a slight decrease in C-balance is observed. In addition, the GC-data of the peracetylated reaction solution reveals only small amounts of THR (Fig. S3 in the ESI†). GC analysis of the gas phase after 4 h of reaction revealed only CH_4 with a C-yield of 24% for Ru/C whereas Ru/CTF-b only gave 8% (Fig. 3). It is proposed that CH_4 is formed from the decarbonylation product CO under high H_2 pressure. CO can also react to form CH_3OH or CO_2; however, CH_3OH was not detected. It is likely that any CO_2 formed will react with the present $Ca(OH)_2$ to $CaCO_3$. Metal carbonates can further react with CO to metal oxalates.[40] The formation of CaC_2O_4 was already observed in the hydrogenolysis of xylitol over Cu/SiO_2.[41] To quantify CO_3^{2-} formation, the reaction solution was acidified and the evolved CO_2 volume measured. Oxalate formation was analysed by HPLC of the acidified solution. For Ru/C, 2% CO_2 in form of $CaCO_3$ was formed, 1% for Ru/CTF-b, whereas CaC_2O_4 could not be observed in either case. For Ru/C a combined yield of C_1-products of 26% can be found whereas for Ru/CTF-b only 9% were formed leading to an improved glycol yield.

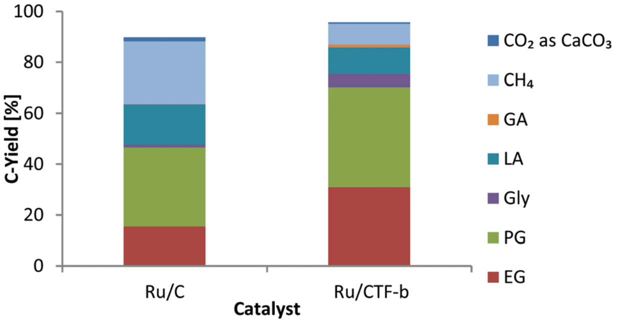

Fig. 3 Liquid, gaseous and solid product yields for the Ru/C and Ru/CTF-b catalysed hydrogenolysis of xylitol (conditions: 473 K, 4 h, 8 MPa H_2, 2.0 g xylitol, 0.2 g catalyst, 0.3 g $Ca(OH)_2$, 20 mL H_2O).

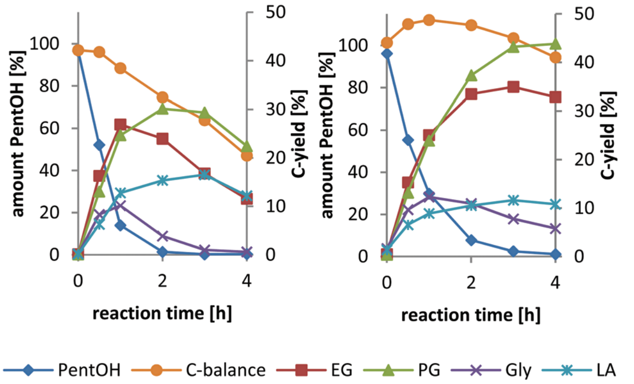

Fig. 2 Time-dependence of the Ru/C (5 wt%)(left) and Ru/CTF-b (right) catalysed hydrogenolysis of xylitol (conditions: 473 K, 8 MPa H_2, 2.0 g xylitol, 0.2 g catalyst, 0.3 g $Ca(OH)_2$, 20 mL H_2O).

Considering the reaction mechanism (Scheme 3), in the first reaction step dehydrogenation takes place yielding adsorbed 1-/5-aldoses or 2-/3-/4-ketoses *via* micro-reversibility.[11] For the 1-/5-aldose (*i.e.* xylose) decarbonylation yields THR, which is observed for Ru/C but not for the Ru/CTF-cata-

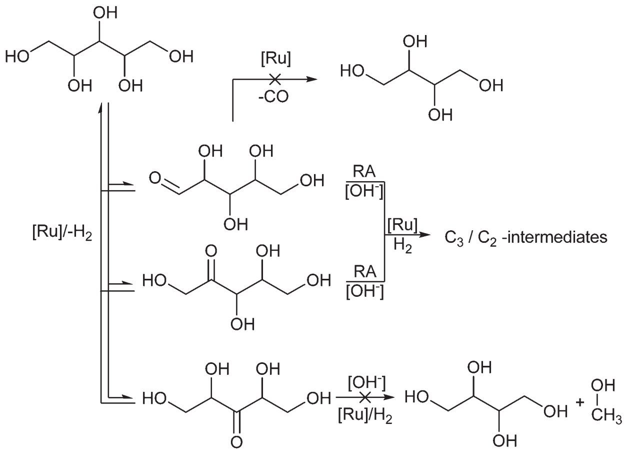

Scheme 3 Proposed reaction mechanism for the hydrogenolysis of pentitols.

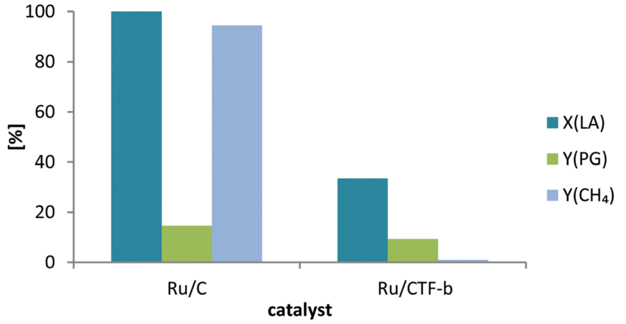

Fig. 4 Lactic acid hydrogenation over Ru/C and R/CTF-b (conditions: 473 K, 4 h, 8 MPa H_2, 0.65 g LA, 0.2 g catalyst, 0.3 g $Ca(OH)_2$, 20 mL H_2O).

lysts. Retro-aldol condensation (RA) of the 1-/5-aldose and 2-/4-ketose leads to C_3 and C_2 intermediates, which after hydrogenation yield GLY and EG. RA of the 3-ketose leads to a C_4/C_1 split forming THR and erythritol in a 1 : 1 ratio; however, the GC data emphasise that this does not occur.

The increased PG selectivity and decreased LA formation for Ru/CTF may be the result of increased LA hydrogenation. To test this we have carried out reactions on LA using Ru/C and Ru/CTF-b (Fig. 4). After 4 h, Ru/C gave full conversion with 15% selectivity to PG and gas phase analysis revealed 94% CH_4 yield (C-balance over 100%). In contrast, Ru/CTF-b only gave 34% conversion with 28% selectivity to PG and only 1% CH_4. These data clearly show that CTF supports can effectively suppress decarbonylation and have a pronounced effect on the selectivity of Ru. However, the higher PG selectivity cannot be attributed to LA hydrogenation. Hence the cause for this effect appears to be due to the electronic structure of the active metal or the presence of nitrogen in the support.

Influence of the Ru-oxidation state

The employed impregnation method leads to a molecular dispersion of Ru on the support. However, hydrogenolysis is carried out at high H_2 pressure and temperature, which are conditions that facilitate nanoparticle formation. This raises the question if the observed selectivity change is the result of metal complexes or a modulation of the reactivity of Ru nanoparticles by the CTF-support. To test this, we have performed a reaction with $[RuCl_2(p\text{-cymene})]_2$ in the presence of 2,2′-bipyridine (3 eq. w.r.t. Ru) as a homogeneous model for CTF-b (Fig. S3 in the ESI†). The data reveal only 20% conversion after 2 h reaction while LA is the main product, indicating that molecular species are much less reactive and selective. In addition, we have studied the influence of the oxidation state of the metal precursor (Fig. 5). CTF-b loaded with $RuCl_3$ gave similar activity and selectivity as $[RuCl_2(p\text{-cymene})]_2$, although the formation of LA was higher at the expense of PG. To obtain a Ru(0) catalyst, the $RuCl_3$ loaded material was reduced under H_2 at 623 K for 3 h ($RuCl_3$-red.). For this catalyst the selectivity to PG was significantly less due to increased formation of LA and GLY.

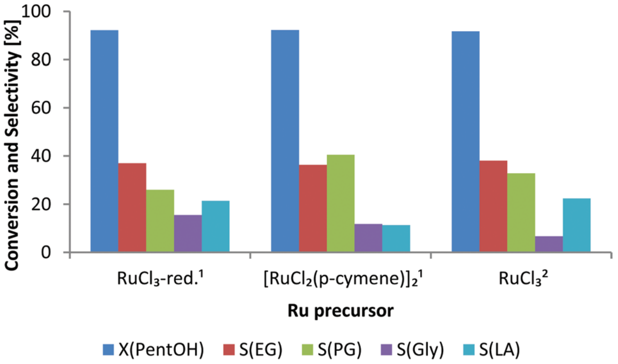

Fig. 5 Conversion and selectivity for Ru/CTF-b using different metal precursors (conditions: 473 K, (1) 2 h, (2) 3 h, 8 MPa H_2, 2.0 g xylitol, 0.2 g catalyst, 0.3 g $Ca(OH)_2$, 20 mL H_2O).

Nevertheless, in all cases the selectivity to EG was comparable and the mass balance approached 100%, indicating suppression of decarbonylation.

Ru nanoparticles

Based on the data above it is proposed that Ru is reduced to nanoparticles during the reaction. To gain more insight into nanoparticle formation on Ru/CTF-catalysts, H_2-chemisorption was performed on the reduced materials (Table 3). The results confirm a clear trend between the active metal surface and the N-content of the support. Going from CTF-d to CTF-b the N-content increases from 3.7% to 17.2% and the accessible Ru surface increases from 1.8 to 8.7 $m^2\ g^{-1}$, respectively. Conversely the calculated crystallite size decreases from 11.1 (cubic)/13.3 (hemispherical) nm to 2.3/2.8 nm. This indicates that a high N-content improves the stabilization of small Ru nanoparticles (*e.g.* by inhibiting sintering). Interestingly, the particles on Ru/C exhibit comparable properties as Ru/CTF-b. Hence it can be concluded that the dramatic difference in selectivity between these catalysts can be attributed to the presence of nitrogen in the support.

Influence of nitrogen in the support

As discussed above, higher yields are obtained for Ru/CTF catalysts due to a suppression of the decarbonylation activity typi-

Table 3 H_2-Chemisorption and elemental analysis results for Ru/CTF-catalysts and Ru/C (samples reduced under H_2-flow at 623 K for 16 h, prior to measurement)

Catalyst	N-Content [%]	Ru surface [$m^2\ g^{-1}$]	Dispersion [%]	Crystal size (cubic/hemispherical) [nm]
Ru/CTF-b	17.2	8.7	26.3	2.3/2.8
Ru/CTF-c	10.4	6.0	18.0	3.4/4.0
Ru/CTF-d	3.7	1.8	5.5	11.1/13.3
Ru/C	0	7.2	21.6	2.8/3.4

cally observed for Ru/C. In addition the selectivity to LA decreases with increasing N-content and active metal surface. This suggests that nitrogen in the support influences not only sintering but also metal particle size. XPS studies were carried out to gain more insight into the influence of the support on the surface chemistry of Ru. Due to the overlapping regions of C 1s and Ru 3d, it was chosen to use N 1s of pyridinic nitrogen at 398.0 eV as reference. This binding energy was confirmed for CTF-b (398.04 eV) and unreduced Ru/CTF-b (398.06 eV) when referenced to C 1s of adventitious carbon (284.5 eV). The data show that Ru-loading does not influence the peak position of the pyridinic N 1s signal (Fig. S5 in the ESI†). Besides this the CTF materials also exhibit pyrollic, graphitic, oxidic, and chemisorbed nitrogen species (Fig. 6a). For the $[RuCl_2(p\text{-cymene})]_2$-loaded CTF-b also four different C species can be found possibly corresponding to the varying C–N bindings while the Ru $3d_{5/2}$ signal is observed at 281.5 eV (Fig. 6b) confirming the Ru(II) state.[42] After reduction (Fig. 6c) the Ru $3d_{5/2}$ signal is observed at 297.7 eV indicating a complete reduction to Ru(0).[42] Compared to the signal of freshly reduced Ru/C (Fig. 6d), which exhibits a binding energy of 280.3 eV for the Ru $3d_{5/2}$ signal, the signal of Ru/CTF-b is shifted 0.6 eV to lower binding energy. We propose that this shift is the result of the donating property of N in the CTF-support. Therefore, these data confirm that the electronic structure of the Ru surface is affected by the CTF support. Besides this the change in selectivity might also be the result of the support itself. As already described in literature, CTF materials exhibit a high surface basicity.[43] Especially pyridinic, pyrollic and graphitic nitrogen species present in the CTF-b material possess lewis basic functions. This way nitrogen affects the local catalyst environment and may possess a high affinity for reaction intermediates. However when considering that the reaction proceeds under strongly basic conditions, we suggest that the electronic effect on Ru is the most likely cause for the suppression of decarbonylation. Moreover it is proposed that the electron donation of N to Ru decreases adsorption energies and facilitates desorption and as a result decreases the occurrence of side reactions.

Catalyst stability

Finally, the stability of Ru/CTF-b was studied over five runs of 1 h (Fig. 7). Activity only slightly decreases over five cycles. Conversion decreases gradually from 80% to 67% and the selectivities to the desired products are comparable in all cases. ICP-OES of the reaction mixtures indicates only minimal leaching which decreases to below the detection limit after 3 runs (Table S1 in the ESI†). TEM images of the spent catalyst reveal well dispersed nanoparticles of 2–3 nm size (Fig. 8). This is similar to the particle size observed by chemisorption and supports the proposition that the CTF-support is able to stabilise metal nanoparticles. These data clearly demonstrate that Ru/CTF-b is a highly active, selective as well as stable catalyst for the hydrogenolysis of xylitol.

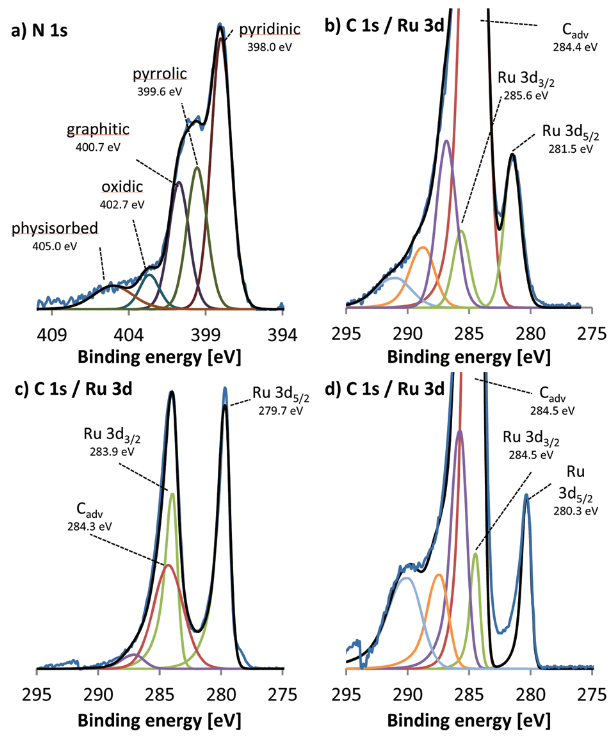

Fig. 6 XPS spectra for (a) N 1s of CTF-b, (b) C 1s and Ru 3d for Ru/CTF-b, (c) C 1s and Ru 3d of reduced Ru/CTF-b, (d) C 1s and Ru 3d for freshly reduced Ru/C (a–c: referenced to N 1s at 398.0 eV, d: referenced to C 1s at 284.5 eV).

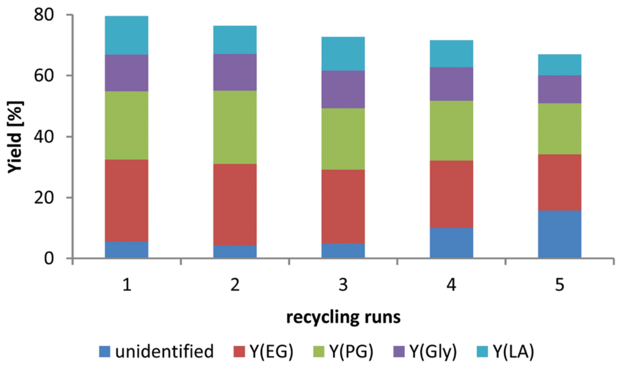

Fig. 7 Recycling of Ru/CTF-b in the hydrogenolysis of xylitol (conditions: 473 K, 8 MPa H_2, 1 h reaction, 2.0 g xylitol, 0.2 g catalyst, 0.3 g $Ca(OH)_2$, 20 mL H_2O).

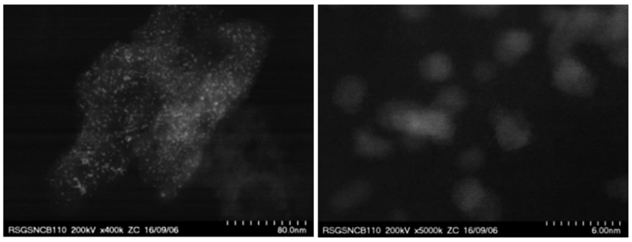

Fig. 8 Dark field TEM-image of the spent Ru/CTF-b catalyst after 5 recycling runs.

Conclusions

In conclusion, Ru/CTF-b presents a highly selective catalyst for the production of glycols from XYL. Up to 80% yield of glycols were obtained in the presence of $Ca(OH)_2$ while successfully suppressing the formation of LA. Variation of the support revealed that the selectivity to EG and PG increases with the nitrogen content of the CTF-support, whereas the selectivity to LA decreases. In contrast to Ru/C, the products are not decomposed (*via* decarbonylation) leading to much higher yields of the desired products. It is proposed that this superior performance of Ru/CTF catalysts results from the Lewis basic support material, which facilitates product desorption from the active metal centre. Also N has a profound impact on the Ru surface chemistry; in XPS the Ru $3d_{5/2}$ signal is shifted to lower binding energy for the reduced sample compared to Ru/C. Furthermore, recycling studies using Ru/CTF-b show a constant activity and selectivity over multiple runs emphasising the stability of the catalyst.

Experimental

All synthesis steps were carried out under inert atmosphere and the catalyst was stored under N_2. Ru/C (5 wt%) was obtained from Sigma-Aldrich and used as delivered. Chemicals were purchased from Abcr ($RuCl_3 \cdot xH_2O$), Chemsolute (HCl, pyridine, THF), Merck (acetic anhydride, $Ca(OH)_2$, NaOH), NORIT (CABOT A SUPRA (activated carbon)), Roth (xylitol) Sigma-Aldrich (4,4′-Biphenyldicarbonitrile, 1,4-dicyano-benzene, $Ni(NO_3)_2 \cdot 6H_2O$, 5 wt% Pt/C, 2,6-pyridinedicarbonitrile, $[RuCl_2(p\text{-cymene})]_2$, $ZnCl_2$), and westfalen (H_2). The catalyst supports were analysed by elemental analysis (2400 CHNS/O Series II System by PerkinElmer), N_2-physisorption (Quadrasorb SI by Quantachrome Instruments), materials were degassed in a FloVac Degasser by Quantachrome Instruments in vacuum at 393 K for at least 4 h and TEM (HD-2700 by Hitachi). ICP-OES was performed on an ICP Spectroflame D by Spectro. H_2-Chemisorption was measured on a 3flex by Micromeritics (prior to measurement the catalysts were reduced under H_2 at 623 K for 16 h). Metal surface, dispersion and crystal size were calculated using the Freundlich and Langmuir models. GC-analysis was performed on a Thermo Scientific Trace GC system equipped with a DB 23 column by Agilent after peracetylation using a mixture of acetic anhydride and pyridine (3 : 1 (v : v), 1 mL per 0.1 mL of reaction solution). HPLC analysis was performed on a Shimadzu system (Rezex ROA-Organic Acid H+ (8%) column by Phenomenex, (eluent: 0.05 M H_2SO_4)). Gas phase GC analysis was performed on an Agilent HP6890 system with a 2 m Shin carbon ST 100/120 mesh micro packed column using a TCD detector. Helium was used as transport gas with a constant flow rate of 24.6 mL min^{-1}. X-ray photoelectron spectroscopy (XPS) measurements were carried out using a Kratos HSi spectrometer with a hemispherical analyser. Reduced samples were prepared and transferred under inert gas atmosphere. The monochromatised Al K_α X-ray source (E = 1486.6 eV) was operated at 15 kV and 15 mA. Binding energies were referenced to N 1s at 398.0 eV and C 1s to 284.5 eV.

CTF-synthesis

Dicarbonitrile (2,6-pyridinedicarbonitrile (CTF-b), 1,4-dicyano-benzene (CTF-c) or 4,4′-Biphenyldicarbonitrile (CTF-d), 4.85 mmol, 1 eq.) was ground with $ZnCl_2$ (24.25 mmol, 5 eq.) and transferred into a quartz ampoule. After drying for 3 h at RT in high vacuum, the ampoule was flame-sealed and placed in a furnace. The ampoule was heated first to 400 K for 10 h and then to 600 K for 10 h. The ampoules were cooled to RT and opened. The black solid was ground and washed with HCl (1 M, 3 L) and dried. The obtained powder was ground using a ball mill (Fritsch Pulverisette 23, 5 min, 30 Hz). The material was washed with dilute HCl (2 M, 0.25 L) and neutralized with water, dilute NaOH (1 M, 0.40 L) and neutralized with water and THF (0.40 L). Drying took place under vacuum for 12 h.

Catalyst preparation

Metal salt $[RuCl_2(p\text{-cymene})]_2$ (106 mg, 0.173 mmol) or $RuCl_3 \cdot xH_2O$ (86.42 mg, 0.346 mmol) and CTF (700 mg) were dispersed in ethanol (200 mL). The suspension was refluxed until the filtrate was clear and colourless. The catalyst was filtered and dried in vacuum at 333 K. The filtrate was concentrated in vacuum and the residue dissolved in H_2O (25 mL) and analysed by ICP-OES. If no clear solution could be found after impregnation, the solvent was evaporated using a rotation evaporator and the catalyst was dried. For the synthesis of $RuCl_3$-red./CTF catalyst reduction under hydrogen took place for 3 h at 623 K (6 L h^{-1}) using a heating rate of 8 K min^{-1}. To obtain the 10 wt% Ni/C catalyst activated carbon CABOT A SUPRA was impregnated with $Ni(NO_3)_2 \cdot 6H_2O$ using the incipient wetness impregnation method. After drying the catalyst was reduced under hydrogen for 2 h at 673 K (6 L h^{-1}) using a heating rate of 5 K min^{-1}.

Catalysis

Hydrogenolysis and hydrogenation reactions were carried out in a 50 mL stainless steel autoclave equipped with a Teflon inlet, a sampling tube. All reactions were performed at 473 K while stirring with a magnetic stirrer at 750 rpm. In a typical experiment, the autoclave was charged with XYL (2.00 g, 13.1 mmol, 1 eq.) or LA (0.65 g, 7.2 mmol, 0.55 eq.), catalyst (0.20 g, 0.1 eq.), $Ca(OH)_2$ (0.30 g, 4.0 mmol, 0.3 eq.) and water (deionized, 20 mL). The autoclave was flushed 3 times using H_2 and pressurized with 8 MPa H_2. Samples were taken periodically and filtered over a syringe filter (PA 45/25). The samples were analysed by HPLC and GC. For the recycling experiments, the catalyst was filtered and washed with aqueous acetic acid (60 mL, 1 M), water (until the washing solution was at pH 7) and ethanol (60 mL). The catalyst was dried in vacuum at 333 K. All steps for catalyst recycling were carried out under N_2 atmosphere.

In case of the homogeneously catalysed reaction, $[RuCl_2(p\text{-cymene})]_2$ (0.049 mmol) and bipyridine (0.085 mmol) were coordinated in EtOH (2.0 mL) and added to a solution of XYL (2.0 g), water (20 mL) and $CaOH_2$ (0.3 g). The reaction was carried out and analysed as described above.

Conflicts of interest

There are no conflicts to declare.

Acknowledgements

We would like to thank Carina Kirstein from the ICVT in Clausthal for chemisorption experiments, Norbert Pfänder from the MPI Mülheim for TEM-images. We thank Noah Avraham, Simon Petring, Heike Bergstein and Elke Biener for HPLC, GC and ICP-OES analyses.

Notes and references

1 R. A. Sheldon, *Catal. Today*, 2011, **167**, 3–13.
2 A. M. Ruppert, K. Weinberg and R. Palkovits, *Angew. Chem., Int. Ed.*, 2012, **51**, 2564–2601.
3 R. Rinaldi, R. Jastrzebski, M. T. Clough, J. Ralph, M. Kennema, P. C. A. Bruijnincx and B. M. Weckhuysen, *Angew. Chem., Int. Ed.*, 2016, **55**, 8164–8215.
4 T. vom Stein, P. M. Grande, H. Kayser, F. Sibilla, W. Leitner and P. Dominguez de Maria, *Green Chem.*, 2011, **13**, 1772–1777.
5 X. Liu, X. Wang, S. Yao, Y. Jiang, J. Guan and X. Mu, *RSC Adv.*, 2014, **4**, 49501–49520.
6 A. Corma, S. Iborra and A. Velty, *Chem. Rev.*, 2007, **107**, 2411–2502.
7 P. Gallezot, *Chem. Soc. Rev.*, 2012, **41**, 1538–1558.
8 T. vom Stein, P. M. Grande, W. Leitner and P. Domínguez de María, *ChemSusChem*, 2011, **4**, 1592–1594.
9 K. Chen, M. Tamura, Z. Yuan, Y. Nakagawa and K. Tomishige, *ChemSusChem*, 2013, **6**, 613–621.
10 S. Liu, Y. Okuyama, M. Tamura, Y. Nakagawa, A. Imai and K. Tomishige, *Green Chem.*, 2016, **18**, 165–175.
11 C. Montassier, D. Giraud and J. Barbier, *Stud. Surf. Sci. Catal*, Elsevier, 1988,pp. 165–170.
12 D. K. Sohounloue, C. Montassier and J. Barbier, *React. Kinet. Catal. Lett.*, 1983, **22**, 391–397.
13 K. Wang, M. C. Hawley and T. D. Furney, *Ind. Eng. Chem. Res.*, 1995, **34**, 3766–3770.
14 M. A. Andrews and S. A. Klaeren, *J. Am. Chem. Soc.*, 1989, **111**, 4131–4133.
15 P. J. C. Hausoul, L. Negahdar, K. Schute and R. Palkovits, *ChemSusChem*, 2015, **8**, 3323–3330.
16 K. L. Deutsch, D. G. Lahr and B. H. Shanks, *Green Chem.*, 2012, **14**, 1635–1642.
17 E. P. Maris and R. J. Davis, *J. Catal.*, 2007, **249**, 328–337.
18 J. Sun and H. Liu, *Green Chem.*, 2011, **13**, 135–142.
19 J. Sun and H. Liu, *Catal. Today*, 2014, **234**, 75–82.
20 R. Sun, T. Wang, M. Zheng, W. Deng, J. Pang, A. Wang, X. Wang and T. Zhang, *ACS Catal.*, 2015, **5**, 874–883.
21 Z. Zhou, S. Dai, J. Qin, P. Yu and W. Wu, *RSC Adv.*, 2015, **5**, 70410–70416.
22 Y. Zhang, A. Wang and T. Zhang, *Chem. Commun.*, 2010, **46**, 862–864.
23 R. Ooms, M. Dusselier, J. A. Geboers, B. Op de Beeck, R. Verhaeven, E. Gobechiya, J. A. Martens, A. Redl and B. F. Sels, *Green Chem.*, 2014, **16**, 695–707.
24 N. Ji, T. Zhang, M. Zheng, A. Wang, H. Wang, X. Wang and J. G. Chen, *Angew. Chem.*, 2008, **120**, 8638–8641.
25 N. Ji, M. Zheng, A. Wang, T. Zhang and J. G. Chen, *ChemSusChem*, 2012, **5**, 939–944.
26 M.-Y. Zheng, A.-Q. Wang, N. Ji, J.-F. Pang, X.-D. Wang and T. Zhang, *ChemSusChem*, 2010, **3**, 63–66.
27 F. Auneau, M. Berchu, G. Aubert, C. Pinel, M. Besson, D. Todaro, M. Bernardi, T. Ponsetti and R. Di Felice, *Catal. Today*, 2014, **234**, 100–106.
28 M. Rivière, N. Perret, A. Cabiac, D. Delcroix, C. Pinel and M. Besson, *ChemCatChem*, 2017, **9**, 2145–2159.
29 L. Zhao, J. H. Zhou, Z. J. Sui and X. G. Zhou, *Chem. Eng. Sci.*, 2010, **65**, 30–35.
30 J. Lee, Y. Xu and G. W. Huber, *Appl. Catal., B*, 2013, **140–141**, 98–107.
31 T. Soták, T. Schmidt and M. Hronec, *Appl. Catal., A*, 2013, **459**, 26–33.
32 C. Montassier, J. C. Ménézo, L. C. Hoang, C. Renaud and J. Barbier, *J. Mol. Catal.*, 1991, **70**, 99–110.
33 S. Tronci and B. Pittau, *RSC Adv.*, 2015, **5**, 23086–23093.
34 W. Shen and W. Fan, *J. Mater. Chem. A*, 2013, **1**, 999–1013.
35 M. Soorholtz, R. J. White, T. Zimmermann, M.-M. Titirici, M. Antonietti, R. Palkovits and F. Schuth, *Chem. Commun.*, 2013, **49**, 240–242.
36 C. Galeano, J. C. Meier, M. Soorholtz, H. Bongard, C. Baldizzone, K. J. J. Mayrhofer and F. Schüth, *ACS Catal.*, 2014, **4**, 3856–3868.
37 P. Kuhn, M. Antonietti and A. Thomas, *Angew. Chem.*, 2008, **120**, 3499–3502.
38 J. Artz, S. Mallmann and R. Palkovits, *ChemSusChem*, 2015, **8**, 672–679.
39 P. J. C. Hausoul, A. K. Beine, L. Neghadar and R. Palkovits, *Catal. Sci. Technol.*, 2017, **7**, 56–63.
40 K. Kudo, F. Ikoma, S. Mori, K. Komatsu and N. Sugita, *J. Chem. Soc., Perkin Trans. 2*, 1997, 679–682.
41 H. Liu, Z. Huang, C. Xia, Y. Jia, J. Chen and H. Liu, *ChemCatChem*, 2014, **6**, 2918–2928.
42 J. F. Moulder, W. F. Stickle, P. E. Sobol and K. D. Bomben, *Handbook of X-ray Photoelectron Spectroscopy*, PerkinElmer Corporation, Eden Prairie, 1992, pp. 114–115.
43 G. Tuci, M. Pilaski, H. Ba, A. Rossin, L. Luconi, S. Caporali, C. Pham-Huu, R. Palkovits and G. Giambastiani, *Adv. Funct. Mater.*, 2017, **27**, 1605672.